Eur. Phys. J. B **27**, 321–327 (2002)
DOI: 10.1140/epjb/e2002-00161-6

THE EUROPEAN PHYSICAL JOURNAL B

Phase diagrams of Ising films with competing interactions

W. Selke[1,a], M. Pleimling[2], and D. Catrein[3]

[1] Institut für Theoretische Physik, Technische Hochschule, 52056 Aachen, Germany
[2] Institut für Theoretische Physik I, Universität Erlangen-Nürnberg, 91058 Erlangen, Germany
[3] LFG Stochastik, Technische Hochschule, 52056 Aachen, Germany

Received 19 March 2002 and Received in final form 2 April 2002
Published online 6 June 2002 –

Abstract. The axial next–nearest–neighbour Ising (ANNNI) model of finite thickness is studied. Using mean–field theory, Monte Carlo simulations, and low–temperature analyses, phase diagrams are determined, with a distinct phase diagram for each film thickness. The robustness of the phase diagrams against varying the couplings in the surface layers is analysed.

PACS. 68.35.Rh Phase transitions and critical phenomena – 75.70.Ak Magnetic properties of monolayers and thin films – 64.70.Rh Commensurate-incommensurate transitions

1 Introduction

In recent years magnetism in thin films of a few atomic layers has attracted much interest, both theoretically and experimentally [1]. However, studies on the influence of the layer thickness, L, on spatially modulated magnetic structures seem to be very scarce [2,3], albeit the possible lack of compatibility between the film geometry and the modulations in the bulk as well as the effect of the surfaces on the ordering phenomena may lead to interesting features.

In this article, we shall deal with this topic by analysing phase diagrams of the axial next–nearest–neighbour Ising (ANNNI) model [4–6] on a simple cubic lattice. Due to its competing interactions, the model displays, in the limit of infinitely many layers, a phase diagram with a plenitude of commensurate phases, including those springing from the multiphase point at zero temperature and those emerging from structure combination branching processes at finite temperatures, as well as incommensurate phases and a Lifshitz point. Many of these aspects have been observed experimentally, in particular in magnets, alloys, polymers, and ferroelectrics, see the reviews [4–6] and related recent work [7–12].

The intriguing structural complexities are severely affected when the lattice consists of rather few layers perpendicular to the axis of competition. Of course, in the case of periodic boundary conditions for the top and bottom layers, the bulk phases which fit to the film thickness still exist [4–6,13]. In the case of free boundary conditions for the surface layers, describing more realistically experimental situations, novel surface–induced features may evolve. The aim of this paper is to identify similarities and typical differences between the phase diagrams in the limit of an infinite lattice and for thin films with free boundaries.

To study the influence of the surfaces in more detail, we also varied the intralayer couplings in the surfaces compared to those in the bulk. In semi–infinite systems, one then encounters the well–known surface critical phenomena with either ordinary or extraordinary and surface phase transitions [14,15], depending on the strength of the surface and bulk couplings. Note that critical properties of the surface magnetization at the Lifshitz point in the semi–infinite ANNNI model have been analysed recently, refining results of mean–field theory [16] by doing Monte Carlo simulations [17].

In the following, we shall mostly deal with thin films of up to ten layers. For each film thickness, distinct phase diagrams in the (temperature–competition strength)-plane are determined, using mean–field theory, low–temperature expansions, and Monte Carlo simulations. Mean–field theory is found to usually provide reliable guidance to the correct phase diagrams; qualitative shortcomings are observed especially in the case of vanishing surface couplings. Brief accounts of some of our findings for equal surface and bulk couplings have been given before [18,19].

The article is organized as follows: first the model and the methods are presented, then the resulting phase diagrams are discussed. The paper is concluded by a summary.

2 Model and methods

We consider the ANNNI model on a simple cubic lattice (setting the lattice constant equal to one) for films of L layers, $L > 2$, with free boundary conditions for the

[a] e-mail: selke@physik.rwth-aachen.de

surface layers. Each spin S_j, at site j, can take only two values, $S_j = 1$ (spin 'up') or $S_j = -1$ (spin 'down'). The interactions are supposed to be ferromagnetic between neighbouring spins in each layer, $J_0 \geq 0$, as well as between neighbouring spins in adjacent layers, $J_1 > 0$, and to be antiferromagnetic, $J_2 < 0$, between axial next–nearest neighbour spins, distinguishing one of the three cubic axes, say, the z–axis. The strength of the competition between the interactions along the z–axis is $\kappa = -J_2/J_1$. The intralayer couplings J_0 may be different in the (top and bottom) surface layers, denoted by J_s, compared to those in the bulk layers, J_b, with the ratio $r = J_s/J_b$. For simplicity, we set $J_b = J_1$. Changing the interlayer coupling J_1 relative to the bulk intralayer interaction, J_b, modifies only quantitatively the phase diagram in the limit $L \longrightarrow \infty$ [20–22].

The ground state properties of the ANNNI films are readily obtained. We first consider $J_s > 0$. The spins in all layers are aligned ferromagnetically at $\kappa < 1/2$. For $\kappa > 1/2$, and even film thickness L, the ground state consists of pairs of layers with, say 'up' spins, denoted as a '2-band' [23,24], followed by a 2–band of 'down' spins, being obviously two–fold degenerate by interchanging the + and − spins. If L is odd, then for $1 > \kappa > 1/2$, the ground state comprises one 3–band and $(L-3)/2$ 2–bands, being $(L-1)$–fold degenerate. For $\kappa > 1$, structures with one 1-band at the surface and 2-bands are stable, with a 4–fold degeneracy. Both for even and odd number of layers L, the degeneracy D_L of the multiphase point at $\kappa = 1/2$ is given by a Fibonacci sequence $D_L = D_{L-1} + D_{L-2}$, where $D_2 = D_3 = 2$, corresponding to all possible combinations of $k-$bands with $k > 1$, as discussed before [24,25]. For L odd, at $\kappa = 1$, $L + 3$ structures have the same ground state energy. For $J_s = 0$, the situation at $\kappa \geq 1$ is of special interest, L being odd. At $\kappa = 1$, structures with 2-bands followed by an arbitrarily ordered surface layer are degenerate, due to the compensation of the interlayer interactions between the surface spins and those in the adjacent and next–nearest layers. In the case of $L = 3$ and $\kappa > 1$, the orientations of the spins in one of the surface layers are random, and completely antiparallel to that random pattern in the other surface; in the center layer, all spins have the same sign.

At non–zero temperatures, the stable phases have been determined using mean–field theory, low–temperature expansions, especially about the special points ($T = 0$, $\kappa = 1/2$) and ($T = 0, \kappa = 1$), as well as Monte Carlo techniques.

In mean–field theory, the magnetization per layer, m_i, $i = 1,2,...L$, in thermal equilibrium follows from the standard equations [20,26–28]

$$m_i = \tanh((4J_0(i)m_i + J_1(m_{i-1} + m_{i+1}) + J_2(m_{i-2} + m_{i+2}))/k_BT) \quad (1)$$

where $J_0(i) = J_s$ for $i = 1, L$ and $J_0(i) = J_b$ for the other layers. Free boundary conditions are implemented by setting $m_i = 0$ for $i = -1, 0, L+1, L+2$. To obtain the thermally stable magnetization pattern, we solved equation (1) iteratively starting from all possible combinations of fully ordered, $m_i = \pm 1$, or completely disordered layers, $m_i = 0$, *i.e.* from, in principle, 3^L distinct configurations (the number may be reduced using symmetry considerations). We then determined among the solutions the one with the lowest free energy. Phase boundaries are identified by singularities in the free energy and specific heat. Obviously, a fine scan of the (temperature k_BT/J_1, competition strength κ)–plane is rather computer–time consuming, and the full analysis of the mean–field theory was done for films of up to $L = 10$ layers. The ratio $r = J_s/J_b$ varied from 0 to 1.5, which would cover, in the limit $L \longrightarrow \infty$, both ordinary and surface transitions.

The transition to the paramagnetic phase may be studied for films of larger thickness, L, by analysing the linearized form of the mean–field theory. From equation (1) one obtains a matrix of rank L, with the eigenvalues determining the phase transition temperature, T_c, and the eigenvectors describing the critical magnetization pattern. Films of thickness up to $L = 50$ were considered, especially for competition ratios close to that of the Lifshitz point in the infinite system, *i.e.* $\kappa = 0.25$.

The phase diagram close to the special ground states at $\kappa = 1/2$ and 1 may be investigated by using exact low–temperature expansions [23,24]. The stable phases are identified by calculating the free energy resulting from spin excitations for all structures being degenerate at the two special points. Indeed, to establish the stable phases springing from the special points for thin films (we studied films with up to ten layers), it usually suffices to do expansions up to first order, involving merely a single spin flip.

Complementary to the low–temperature analysis, Monte Carlo simulations may be applied to study the phase diagrams at higher temperatures. We used both the standard single–flip Metropolis algorithm [29] and a cluster–flip algorithm [30] (attention may be drawn to another cluster–flip algorithm to simulate spatially modulated structures in Ising models [31]). The main aim of our simulations has been to check results of mean–field theory, restricting ourselves to selected cases. Of course, the layers are now finite, consisting of, say, M^2 spins. Thereby, finite–size effects have to be taken into account (here, attention may be drawn to early Monte Carlo work on the nearest neighbour Ising model on thin films [32]). Typically M was varied from 10 to 100. To identify the structures and boundary lines of the various phases, we computed the energy, the specific heat, the layer magnetizations and corresponding histograms as well as correlation functions between spins in different layers. Each run was performed with about 10^6 Monte Carlo steps per spin, when using the single–spin–flip algorithm. In the cluster–algorithm, in each run usually about 2×10^5 clusters were generated.

3 Results

For each film thickness L, distinct phase diagrams are obtained. Before presenting them, we shall outline some general features, as inferred from calculations for films with up to ten layers.

One may distinguish between phases corresponding to ground states and those which are stabilized only at higher temperatures. Especially, the ferromagnetic phase as well as phases consisting of 2–bands augmented, for L odd, by one 3–band or one 1–band, evolve from the ground states. A 'k–band', at $T > 0$, means that spins in k adjacent layers are oriented predominantly in one direction, preceded and followed by layers where the spins are oriented predominantly in the opposite direction. The 3–band tends to be at or near to the center of the film at low temperatures, when it gains entropy from easy spin flips in the two border layers of the 3–band. The band, however, sticks to one of the surfaces of the film when J_s is rather weak so that entropy is gained from energetically easy flips of surface spins, as may be readily seen from low–temperature expansions.

Phases corresponding to ground states with 2–bands and one 3–band at or near the center (or at the surface) of the film may be stabilized only at higher temperatures, due to entropic or symmetrization reasons, while at low temperatures the 3–band sticks to the surface (or center) of the film.

The phases with one 3–band and one 1-band, L odd, are separated, for $J_s > 0$, by the transition line arising from $(T = 0, \kappa = 1)$; the line is at low temperatures of first order. If the surface couplings J_s are not very strong, the line terminates in a critical point, above which the two phases become indistinguishable. That point moves down to zero temperature as J_s vanishes.

Other stable low–temperature phases may spring from the multiphase point ($T = 0$, $\kappa = 1/2$) for $L > 5$. In fact, in the limit $L \longrightarrow \infty$, a sequence of infinitely many periodic $\langle 32^i \rangle$ phases, $i = 0, 1, 2, ..., \infty$, arises from that point (here and in the following, we are using or adapting the standard notation [23,24], setting the sequence of bands in a phase in '$\langle\rangle$'–brackets). For thin films, the low–temperature expansions indicate the following systematics: If L is a multiple of 3, the $\langle 3^{L/3} \rangle$ structures become stable next to the ferromagnetic phase; for $L = 3n + 1 (= 3n + 2)$, $n > 1$, they are replaced by the $\langle 3^{n-1}4 \rangle$ ($\langle 3^{n-1}5 \rangle$) structures. Further phases arising from the multiphase point show up for $L > 7$, having, for $L = 8$, two 3–bands and two 2–bands, and two 3–bands and three 2–bands for $L = 10$. The 3–bands stick to the surfaces of the film, when J_s is sufficiently weak, as before. An increasing number of similar phases comprising 2–bands and 3–bands are expected to occur for thicker films. In comparison to the $\langle 32^i \rangle$ phases, arising from the multiphase point in the limit $L \longrightarrow \infty$, the sequences of 2–bands and 3–bands are slighty rearranged and modified, reflecting the influence of the surfaces.

The transitions between the phases emerging from the multiphase point are, at low temperatures, of first order. Note that, for films, some, but not all these phases extend up to the transition line to the paramagnetic phase, T_c.

Novel phases may become stable close to T_c. As may be obtained readily from the linearized mean–field theory, confirmed by Monte Carlo simulations, the ordered phases directly below this transition line are alternatingly, as κ increases, symmetric and antisymmetric with respect to the center plane (being obviously a real layer for L odd, and a fictitious plane for L even), changing thereby the parity. Each change is associated with an abrupt decrease in the average wavelength, as follows from a Fourier analysis of the magnetization pattern, m_i. For odd L, the magnetization in the center layer vanishes in the antisymmetric cases, denoted as '1_0–band'. There, the interlayer couplings with the neighbouring layers tend to compensate. Such 'partially disordered phases' are, of course not stable below the ordering temperature of the two–dimensional Ising plane. They do not exist in the limit $L \longrightarrow \infty$ [21,22].– Of course, as usual, the location of T_c is largely overestimated in mean–field theory, as seen from comparison with simulational data.

An interesting feature of the transition line to the paramagnetic phase is the point where the ferromagnetic structure becomes unstable against spatially modulated structures, *i.e.* the Lifshitz point in the limit $L \longrightarrow \infty$. In mean–field theory, for rather thick films of up to 50 layers, the surface magnetization is found to show intriguing crossover effects with an effective critical exponent close to 1 in the vicinity of that point, in agreement with the mean–field analysis on the semi–infinite ANNNI model [16]. In a recent Monte Carlo simulation, the exponent has been shown to be significantly affected by critical fluctuations, acquiring a value of about 0.62 [17].

Further phases may show up at intermediate temperatures, in particular, the $\langle 54 \rangle$ and $\langle 64 \rangle$ structures for $L = 9$ and 10. They are reminiscent of the plenitude of commensurate phases on the ferromagnetic side of the ANNNI model in the thermodynamic limit [28], and more of them are expected to occur in thicker films. Likewise, wider films are needed to see indications of the systematic branching processes involving structures with 2–bands and 3–bands, as occurs for $L \longrightarrow \infty$ [28].

Note that the magnetization in a given phase may change sign in some layers when varying temperature and/or strength of couplings, keeping the symmetry of the magnetization pattern about the center plane (symmetric, antisymmetric or asymmetric). For instance, for an (anti–)symmetric phase such a reversal of the sign may happen in the magnetization of the surface layers belonging originally to $k-$bands with $k > 2$, when κ is increased, especially for weak surface couplings. In any event, we characterise a phase by the sequence of bands which occurs at lowest temperatures in case of equal surface and bulk couplings, following the unambiguous notation for the infinite lattice [24].

We shall now discuss results for each film thickness, from $L = 3$ to $L = 10$, illustrating the general features in selected cases in more detail.

In films with three layers, $L = 3$, the ferromagnetic, the $\langle 21 \rangle$ and the $\langle 11_0 1 \rangle$ phases show up. As found in simulations, for equal surface J_s and bulk J_b couplings, the ferromagnetic phase is stable at $\kappa < 1$, the other two phases occur at $\kappa > 1$, with the transition between the $\langle 21 \rangle$ and the partially disordered phases being of second order, see Figure 1, and belonging to the universality class of the

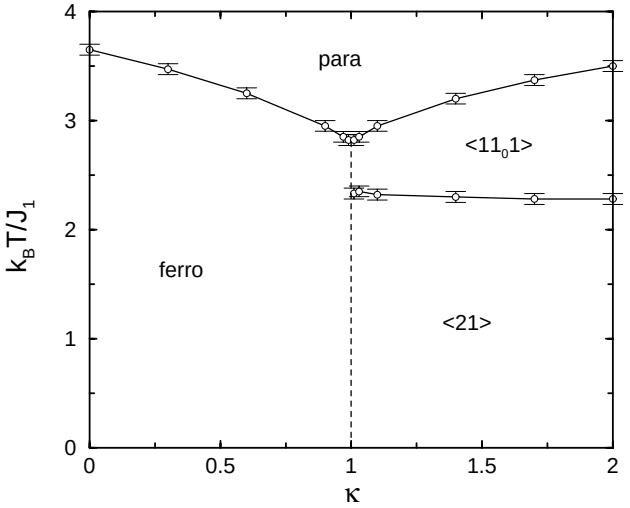

Fig. 1. Phase diagram of the ANNNI model for $L = 3$ and $J_s = J_b$ using Monte Carlo simulations. The curves are guides to the eye. Phase boundaries of first (second) order are denoted by dashed (solid) lines.

two–dimensional Ising model. At $\kappa = 1$, the ferromagnetic and $\langle 21 \rangle$ phases coexist, with the transition being of first order. By weakening the surface interactions, J_s, the ferromagnetic phase extends to larger values of κ, due to the entropic effect in the surface layers. In the limit $J_s = 0$, the $\langle 21 \rangle$ and $\langle 11_0 1 \rangle$ phases are completely suppressed (this aspect is not correctly described in mean–field theory). On the other hand, by enhancing the surface couplings, the $\langle 21 \rangle$ and the $\langle 11_0 1 \rangle$ phases are favoured and stabilized already at $\kappa < 1$, with the transitions to the ferromagnetic phase being always of first order.

For $L = 4$, the phase diagrams are very simple, with two ordered phases, the symmetric, ferromagnetic and the antisymmetric $\langle 2^2 \rangle$ phases being separated by a first order transition line arising from the special point ($T = 0$, $\kappa = 1/2$). By weakening J_s, the range of stability of the symmetric phase is again enlargened. The $\langle 2^2 \rangle$ structure is obviously favoured when the surface layers are more ordered, and thence its range of stability expands when J_s gets stronger.

Somewhat richer phase diagrams are encountered when $L = 5$. For $J_s = J_b$, one finds, increasing the competition ratio κ, at low temperatures the ferromagnetic, the $\langle 32 \rangle$, and the $\langle 2^2 1 \rangle$ phases, with the latter two becoming unstable against the $\langle 21_0 2 \rangle$ and $\langle 131 \rangle$ phases at higher temperatures. Phase diagrams, obtained from mean–field theory and Monte Carlo simulations have been depicted before for the case $J_s = J_b$ [18]. The transition line between the two asymmetric (with respect to the center plane) $\langle 32 \rangle$ and $\langle 2^2 1 \rangle$ phases ends in a critical point above which the phases become essentially indistinguishable. By weakening J_s, the critical point moves to lower temperatures. Eventually, in the limit of zero surface couplings, there is only one asymmetric phase, with one of the surface magnetizations going to zero on approach to $(T = 0, \kappa = 1)$. The phase diagram, as determined from

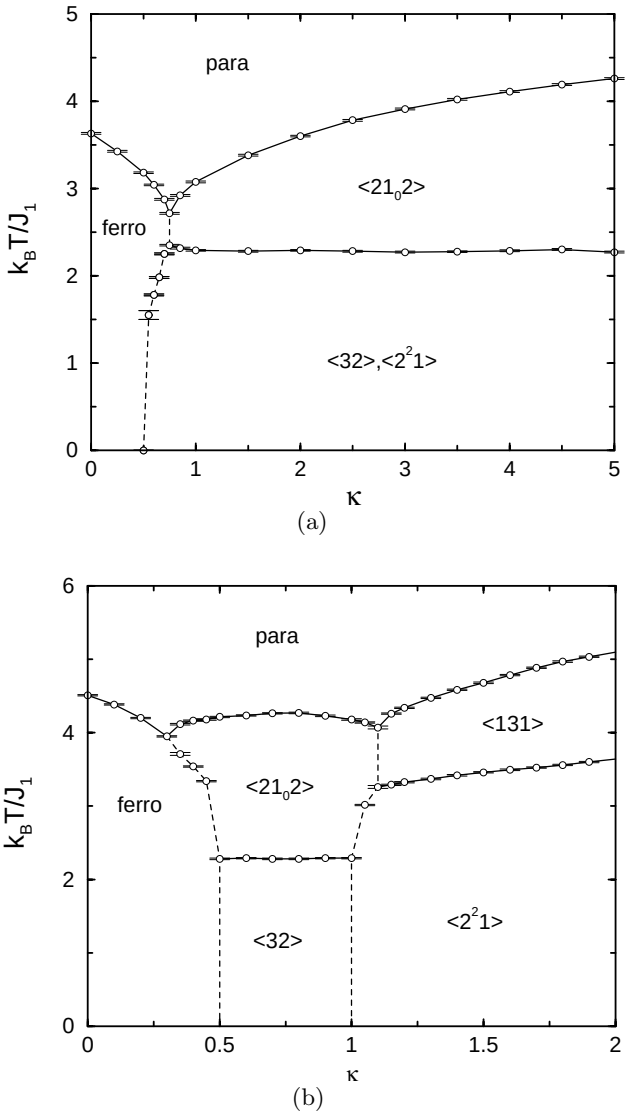

Fig. 2. Simulated phase diagram of the ANNNI model for films with five layers at J_s/J_b= (a) 0 and (b) 1.5.

simulations, is shown in Figure 2a. Note that the $\langle 131 \rangle$ structure, being present close to T_c in the mean-field calculations, is squeezed out (as we checked for κ as large as 15). In turn, the range of stability of the $\langle 21_0 2 \rangle$ phase is underestimated in mean–field theory, similar to the situation for equal surface and bulk couplings [18]. The magnetic disorder in the center layer sets in roughly at the transition temperature of the two–dimensional Ising model, because then the interlayer couplings J_1 and J_2 to the axial spins in the two adjacent and two next–nearest layers are largely cancelled. When increasing the surface couplings J_s, the $\langle 131 \rangle$ phase is stabilized, as shown in Figure 2b, in qualitative agreement with mean–field theory. Actually, the magnetization then tends to be close to zero in the second and fourth layers, being rather large with the same sign in the surface layers and with the opposite sign in the center layer.

For $L = 6$, only three ordered structures exist, the ferromagnetic, the $\langle 3^2 \rangle$, and the $\langle 2^3 \rangle$ phases. The transitions between them are of first order. By decreasing the surface interactions, the range of stability of the $\langle 3^2 \rangle$ phase gets wider, with 1-bands at the surfaces for large competition ratio κ. This range and that of the ferromagnetic phase shrink when enhancing the surface couplings, and the $\langle 2^3 \rangle$ structure is favoured. Predictions of mean–field theory were qualitatively confirmed in simulations.

Adding another layer to the film, $L = 7$, leads to quite different phase diagrams, with possibly seven distinct ordered phases, namely the ferromagnetic, $\langle 43 \rangle$, $\langle 31_0 3 \rangle$, $\langle 232 \rangle$, $\langle 32^2 \rangle$, $\langle 2^3 1 \rangle$, and $\langle 121_0 21 \rangle$ phases, as found in mean–field theory. For $J_s = J_b$, the $\langle 232 \rangle$ phase extends down to zero temperature at $1/2 < \kappa < 1$, while the $\langle 32^2 \rangle$ structure is stabilized only at intermediate temperatures, where the entropic effect of the small surface magnetization plays the crucial role [18]. Examples of phase diagrams for different surface and bulk couplings are depicted in Figures 3a and b, for $r = J_s/J_b = 0.25$ and 1.5, as obtained from mean–field theory. Compared to the case of $J_s = J_b$, the enhancement or weakening of the surface couplings may lead to similar trends as for $L = 5$, but also to novel features. As before, when $J_s = 0$, there is no transition line arising from the special point $(T = 0, \kappa = 1)$, *i.e.* the two asymmetric $\langle 32^2 \rangle$ and $\langle 2^3 1 \rangle$ structures transform gradually into each other at non–zero temperatures, with a vanishing magnetization in one of the surface layers on approach to the special point. Indeed, even the transition line to the neighbouring asymmetric $\langle 43 \rangle$ phase terminates in a critical point, above which all these asymmetric structures belong to the same phase. Perhaps somewhat unexpectedly, at $1/2 < \kappa < 1$, the $\langle 32^2 \rangle$ structure forms the low–temperature phase when $r < (3 + \kappa)/4$, while for stronger surface couplings the symmetric $\langle 232 \rangle$ phase is stable down to zero temperature. In the former case, the symmetric phase is stable next to T_c, see Figure 3a. A similar entropy–driven shift of the 3–band from the interior of the film to one of its surfaces occurs at wider films, L odd, as well, for sufficiently weak J_s. The effect follows from the low–temperature analysis, and it is described correctly by mean–field theory.

In the case of $L = 8$, six ordered phases are observed; the phase diagram as obtained from mean–field theory for equal couplings $J_s = J_b$ has been shown before [18]. Apart from the trivial ferromagnetic and $\langle 2^4 \rangle$ phases, there is the $\langle 3^2 2 \rangle$ phase, which may, at sufficiently strong surface couplings J_s, arise from the multiphase point $(T = 0, \kappa = 1/2)$, with the symmetric $\langle 323 \rangle$ structure, formed at higher temperatures, remaining stable up to the transition line to the paramagnetic phase, T_c. The latter phase is stable down to the multiphase point for sufficiently weak surface couplings, where entropy is gained, again, from 3–bands at the surfaces, as follows from low–temperature considerations, in agreement with mean–field calculations. Actually, for small J_s, the $\langle 323 \rangle$ phase persists even for quite large values of the competition ratio κ. Furthermore, the $\langle 53 \rangle$ phase may spring from the multiphase point. The antisymmetric $\langle 4^2 \rangle$ phase is stable close to T_c, extending down to lower temperatures with decreasing surface couplings.

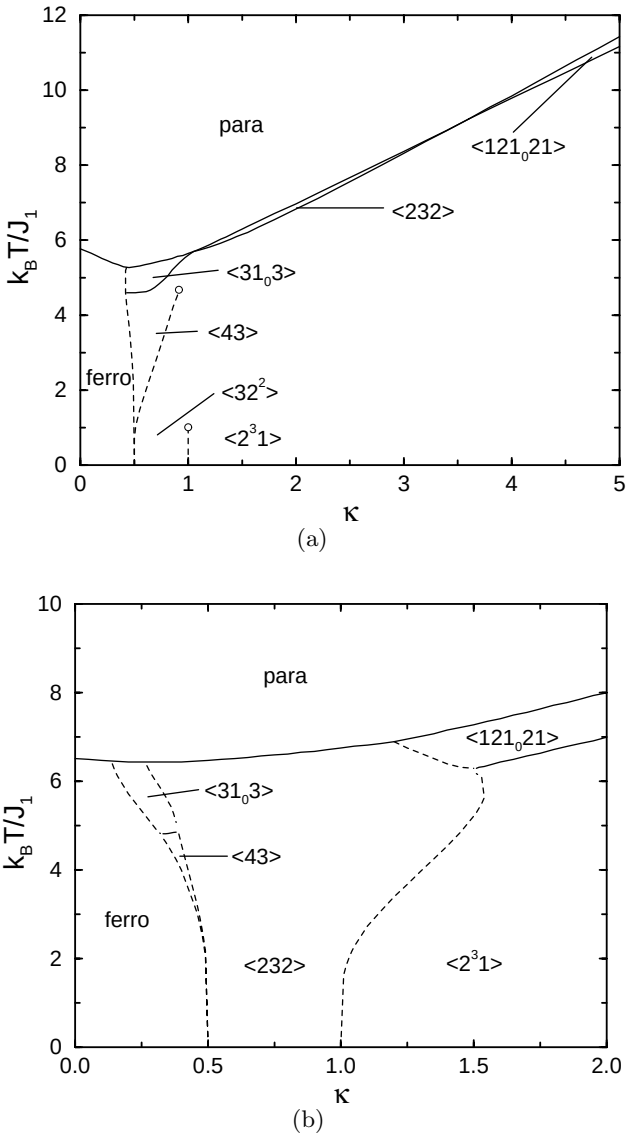

Fig. 3. Phase diagram of the ANNNI model for $L = 7$ at J_s/J_b= (a) 0.25 and (b) 1.5, as obtained from mean–field theory. The critical point at the end of a line of transitions of first order is denoted by an open circle.

In the case of nine layers, the rather complex phase diagrams consist of up to nine ordered phases. Close to T_c, increasing κ, the alternatingly symmetric and antisymmetric phases are the ferromagnetic, $\langle 41_0 4 \rangle$, $\langle 3^3 \rangle$, $\langle 2^2 1_0 2^2 \rangle$, and $\langle 12321 \rangle$ phases. At low temperatures, one may, in addition, encounter, the $\langle 2^4 1 \rangle$ phase as well as, for fairly weak surface couplings, $r < (3 + \kappa)/4$, the $\langle 32^3 \rangle$ phase, and, for stronger couplings, the $\langle 2^2 32 \rangle$ phase at $1/2 < \kappa < 1$, similar to the situation in the case $L = 7$. Again, this feature follows from the low–temperature analysis, and it is described correctly by mean–field theory, see Figure 4 (the case $J_s = J_b$ has been depicted before [19];

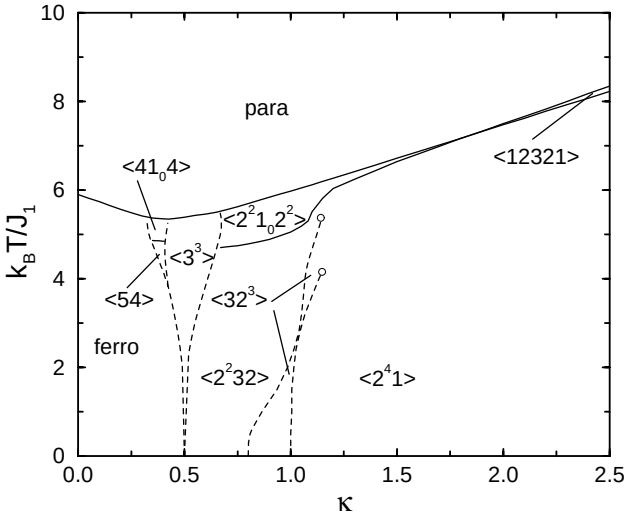

Fig. 4. Phase diagram of the ANNNI model for $L = 9$ at $J_s/J_b = 0.95$ using mean–field theory.

there, the $\langle 32^3 \rangle$ phase is squeezed out). Thence, by lowering the surface couplings, the 3–band eventually sticks at the surface. In fact, the same phenomenon holds for wider odd films as well. The transition line, separating the structures with one 1–band from that with one 3–band and arising from $(T = 0, \kappa = 1)$, terminates again in a critical point for moderate and weak surface couplings. The point moves to zero temperature as J_s vanishes. Perhaps most interestingly, mean–field theory suggests that the $\langle 54 \rangle$ phase is stable at intermediate temperatures, as shown in Figure 4. Indeed, its existence has been confirmed in Monte Carlo simulations for equal surface, J_s, and bulk, J_b, couplings. The phase shows up below the $\langle 41_04 \rangle$ phase which, in turn, becomes stable at about the transition temperature of the two–dimensional Ising model, like the corresponding partially disordered phases for films with an odd number of layers.

Finally, for $L = 10$, seven distinct ordered phases have been identified and located applying mean–field theory for $J_s = J_b$ [19]. Close to the transition to the paramagnetic phase, T_c, the ferromagnetic, $\langle 5^2 \rangle$, $\langle 343 \rangle$, $\langle 23^2 2 \rangle$, and $\langle 2^5 \rangle$ phases occur. The $\langle 43^2 \rangle$ phase springs from the multiphase point $(T = 0, \kappa = 1/2)$. At intermediate temperatures, the $\langle 64 \rangle$ phase has been detected in a tiny region of the phase diagram. The phase persists, when varying the surface couplings. For sufficiently small values of J_s, the $\langle 32^2 3 \rangle$ phase is stabilized, at the cost of the $\langle 23^2 2 \rangle$ phase, near the multiphase point, reflecting again the gain of entropy due to easy excitations of surface spins belonging to 3–bands for structures comprising 3–bands and 2–bands.

4 Summary

The ANNNI model on thin films has been studied, using mean–field theory, low–temperature analyses, and Monte Carlo techniques. For each film thickness, varying the number of layers from $L = 3$ to $L = 10$, distinct phase diagrams have been determined, monitoring surface–induced features by also changing the strength of the couplings in the surface layers.

In the limit of infinite lattices, $L \longrightarrow \infty$, the competing interactions of the ANNNI model lead to a phase diagram with a rich variety of spatially modulated magnetic structures. Signatures of some of these features, like the sequence of commensurate phases springing from the multiphase point, are already present in thin films, with the films displaying generic and distinct features as well. In particular: (i) The ordered phases occuring directly below the transition line to the paramagnetic phase are alternatingly, as the ratio $\kappa = -J_2/J_1$ between the competing interactions of the model increases, symmetric and antisymmetric about the center of the film, leading to partially disordered phases with a paramagnetic center plane for films with an odd number of layers. (ii) The phases springing from the multiphase point may include structures consisting not only of 2–bands and 3–bands, but also with a 4–band or a 5–band. (iii) For L odd, there is an additional transition line near $\kappa = 1$, separating phases with 2–bands augmented by one 3–band or one 1–band.

By modifying the surface couplings, additional interesting phenomena are induced. Indeed, the range of stability of the various phases as well as the type of phase transition may be affected by varying the couplings. Entire transition lines may, in fact, disappear. Perhaps most noticeable, 3–bands may be forced to stick to the surface or move to the interior of the film, thereby possibly forming new phases with a different symmetry.

These findings may encourage experimental work on thin films of magnets or alloys showing complicated spatial orderings in the bulk. On the theoretical side, several extensions of the present study seem to be promising, including the effects of a larger number of layers, modified interactions [33–36], and magnetic bulk as well as surface fields, in order to possibly detect additional systematics in the intriguing phase diagrams of the ANNNI model and variants.

We would like to thank A. Gödecke for useful discussions.

References

1. U. Gradmann, J. Magn. Magn. Mater. **100**, 481 (1991); P. Poulopoulos, K. Baberschke, J. Phys. Cond. Matt. **11**, 9495 (1999)
2. R.A. Cowley, P.M. Gehring, D. Gibbs, J.P. Goff, B. Lake, C.F. Majkrzak, A. Vigliante, R.C.C. Ward, M.R. Wells, J. Phys. Cond. Matt. **10**, 6803 (1998)
3. C. Sutter, D. Labergerie, A. Remhof, H. Zabel, C. Detlefs, G. Grübel, Europhys. Lett. **53**, 257 (2001)
4. W. Selke, Phys. Rep. **170**, 213 (1988)
5. J.M. Yeomans, Adv. Phys. **41**, 151 (1988)
6. B. Neubert, M. Pleimling, R. Siems, Ferroelectrics **208**, 141 (1998)
7. C. Colinet, A. Pasturel, J. Alloy Compd. **319**, 154 (2001)

8. D. Schobinger–Papamantellos, G. Andre, J. Rodriguez–Carvajal, O. Moze, W. Kockelmann, L.D. Tung, K.H. Buschow, J. Magn. Magn. Mater. **231**, 162 (2001)
9. S. Tanaka, M. Yamashita, Ferroelectrics **245**, 881 (2000)
10. G. Martinez, J.R. Iglesias, C. Lacroix, B. Coqblin, Physica B **281**, 440 (2000)
11. D. Schwahn, K. Mortensen, H. Frielinghaus, K. Almdahl, Phys. Rev. Lett. **82**, 5056 (1999)
12. M. Quilichini, J.M. Perez-Mato, I. Aramburu, O. Hernandez, Eur. Phys. J. B **25**, 431 (2002)
13. M. Waasner, A. Hüller, in preparation
14. K. Binder, in *Phase Transitions and Critical Phenomena*, Vol. 8, edited by C. Domb, J.L. Lebowitz (Academic Press, London, and New York, 1983)
15. H.W. Diehl, Int. J. Mod. Phys. B **11**, 3503 (1997)
16. K. Binder, H.L. Frisch, Eur. Phys. J. B **10**, 71 (1999)
17. M. Pleimling, Phys. Rev. B **65**, 184406 (2002)
18. W. Selke, D. Catrein, M. Pleimling, J. Phys. A **33**, L459 (2000)
19. W. Selke, M. Pleimling, I. Peschel, M. Kaulke, M.–C. Chung, D. Catrein, J. Magn. Magn. Mater. **240**, 349 (2002)
20. C.S.O. Yokoi, M.D. Coutinho–Filho, S.R. Salinas, Phys. Rev. B **24**, 4047 (1981)
21. K. Nakanishi, J. Phys. Soc. Jpn **62**, 3789 (1992)
22. F. Rotthaus, W. Selke, J. Phys. Soc. Jpn **61**, 2901 (1993)
23. M.E. Fisher, W. Selke, Phys. Rev. Lett. **44**, 1502 (1980)
24. M.E. Fisher, W. Selke, Phil. Trans. R. Soc. **302**, 1 (1981)
25. S. Redner, J. Stat. Phys. **45**, 587 (1982)
26. T. Janssen, J.A. Tjon, J. Phys. A **16**, 673 (1983)
27. P. Bak, Rep. Prog. Phys. **45**, 587 (1982)
28. W. Selke, P.M. Duxbury, Z. Phys. B **57**, 49 (1984)
29. D.P. Landau, K. Binder, *A Guide to Monte Carlo Simulations in Statistical Physics* (Cambridge, University Press, 2000)
30. M. Pleimling, M. Henkel, Phys. Rev. Lett. **87**, 125702 (2001); M. Henkel, M. Pleimling, Comp. Phys. Commun. (in print) and `cond-mat/0108454`
31. F. Matsubara, T. Shirakura, J. Phys. Soc. Jpn **69**, 178 (2000)
32. K. Binder, Thin Solid Films **20**, 367 (1973)
33. M. Grousson, G. Tarjus, P. Viot, Phys. Rev. E **62**, 7781 (2000)
34. V. Massidda, Physica B **307**, 265 (2001)
35. Y. Muraoka, Phys. Rev. B **64**, 134416 (2001)
36. D. Allen, P. Azaria, P. Lecheminant, J. Phys. A **34**, L305 (2001)